Dynamics of the Euler Buckling Instability

Leonardo Golubović, Dorel Moldovan, and Anatoli Peredera
Physics Department, West Virginia University, Morgantown, West Virginia 26506
(Received 5 February 1998)

We study the dynamics of the classical Euler buckling instability of compressed objects such as flexible molecular chains and thin rods. We reveal that this dynamics is a coarsening process self-similar in time. We relate this process to phase ordering phenomena such as spinodal decomposition. [S0031-9007(98)07392-X]

PACS numbers: 46.30.Lx

Solids under externally applied stresses and strains exhibit a variety of instabilities. A classical example is the well known Euler buckling instability of a compressed rod that buckles out sideways, if the compressional strain ϵ exceeds the critical value $\epsilon_c \sim L^{-2}$; L is the length of the rod [1,2]. Buckling of thin rods and plates is a common phenomenon in engineering practice and diverse branches of materials science [1–5]. For example, buckling instability of polymerized monolayers of insoluble amphiphiles adsorbed at the air-water interface has been observed in recent experiments [4]. Buckling can be induced in a variety of ways, for example, simply by applying a compressional lateral strain to a membrane. In practice, strains causing buckling are frequently of a thermal origin [5]. Rods with hinged ends immersed in a fluid may buckle, if the temperature of the fluid is raised. The temperature jump would expand a rod with free ends. It thus effectively induces a uniform compressive strain ϵ in a rod with fixed ends. If $\epsilon > \epsilon_c \sim L^{-2}$, such a thermally strained rod will buckle.

Historically, Euler buckling instability is the very first example for bifurcation phenomena and paradigm for subsequent theories of phase transition. Still, the dynamics associated with this phenomenon has not been addressed in depth. In itself, buckling involves a spontaneous symmetry breaking. Thus, a compressed membrane may buckle either up or down (breaking of Z_2, Ising-type symmetry), whereas a compressed molecular chain may buckle out sideways in an arbitrary direction (breaking of the O_2 symmetry for rotations around the initial direction of the chain). So, buckling is a practically interesting analog of the *phase ordering phenomenon.* Here we elucidate, for the first time in depth, the nature of the *dynamics of buckling phenomena.* We investigate *how* initially straight, compressionally strained molecular chains evolve into the final buckled shape. We study this evolution by molecular dynamics (MD) simulations of a flexible chain of molecules ("tethered chain"). We find that the evolving chain's profile is like a wave characterized by a wavelength that grows, via a coarsening process, as a power of time. The amplitude (transverse width) of this wavelike chain pattern also grows as a power of time. We find that the dynamics of Euler instability is closely related in its nature to *phase ordering processes* such as spinodal decomposition [6–8]. Interestingly, the growth of the chain's transverse width makes this phenomenon strikingly similar to the interfacial coarsening processes recently found to occur in molecular beam epitaxy [9–11].

As the dynamics associated with buckling instabilities has not been studied in depth, it is natural to focus on the most common of all of the systems exhibiting such instability, that is, the original Euler case of thin rods [1,2] and closely related flexible chain molecules [12]. The dynamical model studied here by MD is the standard Rouse dynamics,

$$\Gamma \frac{d\mathbf{R}_n}{dt} = -\frac{\partial U}{\partial \mathbf{R}_n} + \eta_n(t), \tag{1}$$

of a molecular chain ("molecular rod") moving in a viscous medium. Here $\mathbf{R}_n(t)$ is the position of the nth molecule, Γ is a viscous friction coefficient, and $\eta_n(t)$ is thermal noise. In (1), the chain potential energy $U = U_{\text{com}} + U_{\text{bend}}$, with the compressional energy $U_{\text{com}} = \sum_n \Phi(|\mathbf{R}_{n+1} - \mathbf{R}_n|)$, and the bending energy $U_{\text{bend}} = \frac{1}{2}\sum_n \kappa(\hat{\mathbf{t}}_{n+1} - \hat{\mathbf{t}}_n)^2$; here $\hat{\mathbf{t}}_n = (\mathbf{R}_n - \mathbf{R}_{n-1})/|\mathbf{R}_n - \mathbf{R}_{n-1}|$ are the tangent unit vectors. The bonding potential $\Phi(|\mathbf{R}_{n+1} - \mathbf{R}_n|)$ is minimal, when $|\mathbf{R}_{n+1} - \mathbf{R}_n|$ is equal to the bond length $= 1$. We used $\Phi(|\mathbf{R}_{n+1} - \mathbf{R}_n|) = Be_n^2/2$, where e_n is the *internal* strain $e_n = |\mathbf{R}_{n+1} - \mathbf{R}_n| - 1$. To discuss the chain dynamics, let us split the position vector of the nth molecule $\mathbf{R}_n$ into the transverse part $\mathbf{R}_T(n,t)$ ("undulations"), perpendicular to the initial straight chain direction, and the longitudinal part $R_L(n,t)$, along the initial chain direction. Chain ends are fixed (hinged), and at $t = 0$ the chain was in a compressed, straight configuration. That is, $R_L(n, t = 0) = (1 - \epsilon)n$, and $\mathbf{R}_T(n, t = 0) = 0$. In our simulations we used a 10% compressional external strain, that is, $\epsilon = 0.10$, whereas $B = 1.0$, $\kappa = 0.2$, and $\Gamma = 0.5$.

We focus here on the dynamics without thermal noise ["zero-temperature" dynamics], i.e., we set $\eta_n = 0$ in (1) [13]. The only randomness used here was small *initial* random transverse displacements around the straight unstable equilibrium configuration (to enable chain start moving). Subsequently, buckling instability, due to negative internal strains, amplifies transverse displacements

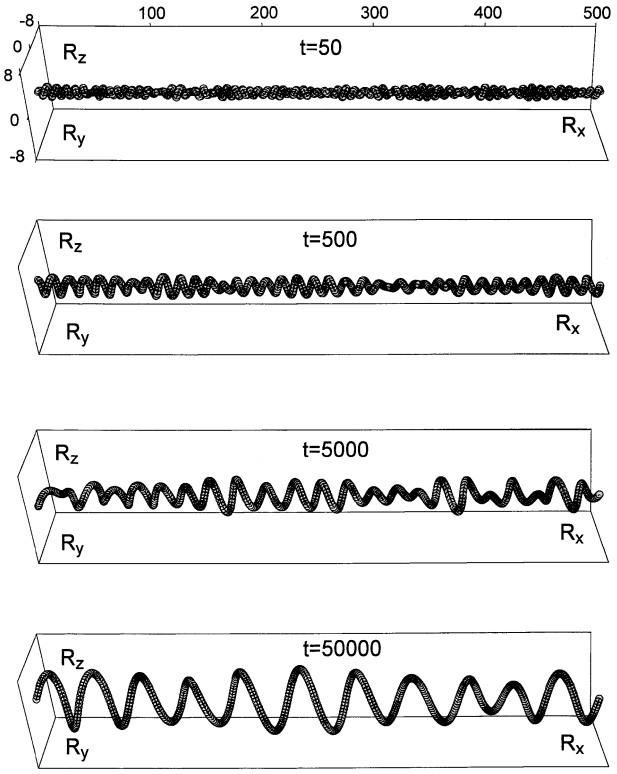

FIG. 1. Time evolution of the molecular chain. We depict some 550 out of $N = 10\,000$ molecules composing the chain. To depict undulations $\mathbf{R}_T$ clearly, we used different scales for the transverse $\mathbf{R}_T = (R_y, R_z)$ and longitudinal $R_L = R_x$ molecular coordinates.

and produces a chaotic dynamics depicted in Fig. 1. Manifestly, chains's transverse displacements $\mathbf{R}_T(n,t)$ develop an *evolving* wavelike pattern characterized by a *time-dependent* structural length scale λ ("wavelength"). This λ grows with time via a *coarsening* process. Associated with this coarsening is a growth of the chain's transverse spread $w(t)$ ("width"); see Fig. 1. $w(t)$ we quantified as $[w(t)]^2 = \langle[\mathbf{R}_T(n,t)]^2\rangle$. Here and in the following, $\langle\,\rangle$ stands for the spatial average defined for any quantity $A(n,t)$ as $\langle A(n,t)\rangle = (1/N)\sum_n A(n,t)$. Chain wavelength $\lambda(t)$ we extracted from the zeros of displacement correlation functions which have a strong oscillatory character reflecting wavelike patterns in Fig. 1. We illustrate this in Fig. 2(a) which depicts the "slope-slope" correlation function $K_{ss}(r,t) = \langle \mathbf{V}_T(n+r,t)\mathbf{V}_T(n,t)\rangle$ with $\mathbf{V}_T(n,t) = \mathbf{R}_T(n+1,t) - \mathbf{R}_T(n,t)$. The wavelength $\lambda(t)$ can be extracted from the first zero $r_1(t)$ of $K_{ss}(r,t)$, via the relation $\lambda(t) = 4r_1(t)$ [which can be rationalized by calculating K_{ss} for $R_T(n,t)$ in the form of a simple harmonic wave with wavelength $\lambda(t)$].

We thus find that, at *long times,*

$$\lambda(t) \sim t^{n_c}, \tag{2}$$

and

$$w(t) \sim t^{\beta}, \tag{3}$$

with the exponents n_c and β *both* nearly equal to 0.26

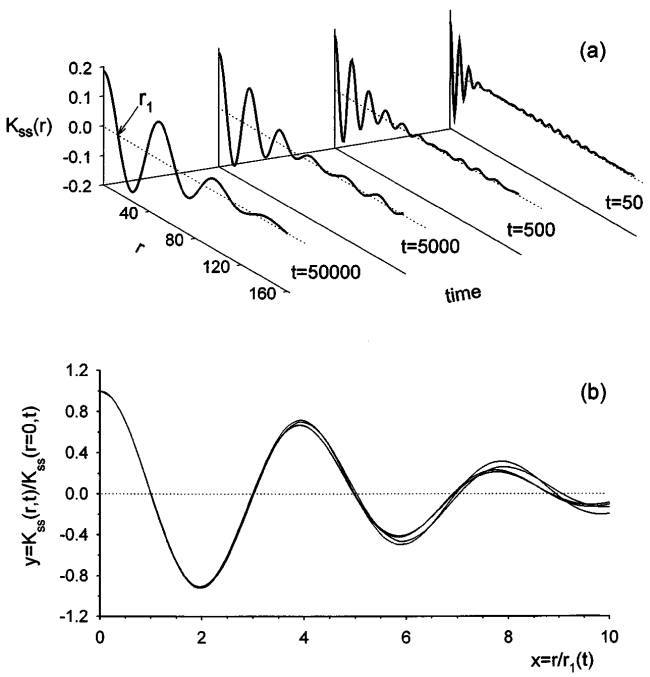

FIG. 2. (a) Slope-slope correlation function $K_{ss}(r,t)$ vs r for various times t. Note that as $t \to \infty$, $K_{ss}(r=0,t) \to 2\epsilon$ $(= 0.2$ here). (b) Self-similarity test for $K_{ss}(r,t)$. Collapse into a single curve $y = \psi(x)$ of the curves in (a). Here $y = K_{ss}(r,t)/K_{ss}(r-0,t)$, and $x = r/r_1(t)$, where $r_1(t)$ is the first zero of $K_{ss}(r,t)$.

from simulations of a 3D chain of $N = 10\,000$ molecules. We obtain additional insight into this scaling behavior by considering the chain's *total* potential energy U which is the sum of the compressional $U_{\rm com}$ and the bending energy $U_{\rm bend}$. Figure 3(a) depicts energies U, $U_{\rm com}$, and $U_{\rm bend}$ vs time. We see that, at *long times,*

$$U_{\rm bend}(t) \sim \frac{1}{t^{\delta}}, \tag{4}$$

with $\delta = 0.50(4)$, whereas

$$U_{\rm com}(t) \sim \frac{1}{t^{\eta}}, \tag{5}$$

with $\eta = 1.02(2)$. As $\eta > \delta$, the net potential (elastic) energy U is, at long times, entirely in the bending energy, $U \approx U_{\rm bend} \gg U_{\rm com}$; see Fig. 3(a). Figure 3(b) depicts the time evolution of the spatial average of the internal strain $e_n(t)$. $\langle e_n\rangle < 0$ as the chain is in a compressed configuration for any t. By Fig. 3(b), for long times, the internal strain relaxes as

$$\langle e_n\rangle \sim -\frac{1}{t^{\gamma}}, \tag{6}$$

with $\gamma = 0.51(1)$. Note that, within the accuracy, one has the scaling relation $\eta = 2\gamma$, where η is the exponent of the compressional energy decay, Eq. (5). This can be easily rationalized as $U_{\rm com} \sim \langle e_n^2\rangle$, if one further assumes that $\langle e_n^2\rangle \sim \langle e_n\rangle^2$.

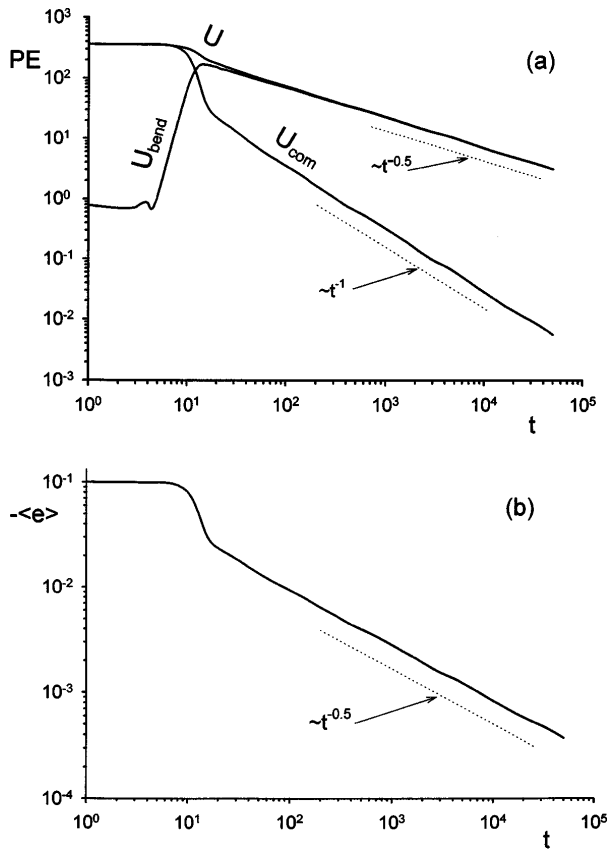

FIG. 3. (a) Evolution of the chain total potential energy $U = U_{\text{bend}} + U_{\text{com}}$, bending energy U_{bend}, and compressional energy U_{com} vs time t. (b) Evolution of the internal strain $\langle e \rangle$ vs time t.

There is an apparent *self-similarity* we see in the chain dynamics. Indeed, from Fig. 1, we infer that chain configurations obtained at *different* long times look (statistically) the *same*, provided transverse displacements $R_T(n,t)$ are expressed in units of $w(t)$ [i.e., in terms of the "dimensionless" quantity $R_T(n,t)/w(t)$], and n is expressed in units of $\lambda(t)$ [i.e., in terms of the dimensionless quantity $n/\lambda(t)$]. Qualitatively speaking, one can say that chain configurations depicted at various times in Fig. 1 are *all* of the form

$$\frac{R_T(n,t)}{w(t)} \approx \sin\left(2\pi\,\frac{n}{\lambda(t)}\right), \tag{7}$$

that is, $y = R_T(n,t)/w(t)$ is a wavelike function of $x = n/\lambda(t)$, with the period $\Delta x = 1$. Statistical self-similarity can be checked by using the slope-slope correlation function $K_{ss}(r,t)$ obtained at various times t; see Fig. 2(a). The slope vector $\mathbf{V}_T(n,t) = \partial \mathbf{R}_T/\partial n$ has the characteristic value $v(t) = w(t)/\lambda(t)$, inferred by looking at a typical chain configuration in Eq. (7). In the spirit of statistical self-similarity, correlation of $\mathbf{V}_T(n,t)/v(t)$ with $\mathbf{V}_T(n+r,t)/v(t)$ should be a function of $r/\lambda(t)$ only, that is,

$$\frac{K_{ss}(r,t)}{v^2(t)} = f_{ss}\left(\frac{r}{\lambda(t)}\right), \tag{8}$$

where $f_{ss}(x)$ is a scaling function. Thus, in particular,

$$K_{ss}(r=0,t) = \langle (\mathbf{V}_T)^2 \rangle = \left\langle \left(\frac{\partial \mathbf{R}_T}{\partial n}\right)^2 \right\rangle = v^2(t) f_{ss}(0)\,. \tag{9}$$

From our simulations, we see that $K_{ss}(r=0,t)$ saturates to a finite value at long times. See Fig. 2(a) at $r = 0$. This feature can be rationalized in terms of Eq. (9), as $v(t) = w(t)/\lambda(t)$, and w and λ are *both* $\sim t^{0.25}$ at *long* times. This is further discussed below, where we find $K_{ss}(r=0,t) = \langle (\partial \mathbf{R}_T/\partial n)^2 \rangle \approx 2\epsilon$ for $\epsilon \ll 1$, at long times. Thus, the self-similarity of $K_{ss}(r,t)$ is simply the statement that, at long times, all the curves in Fig. 2(a) are identical up to a time-dependent rescaling along the r axis *only*. This feature makes the present system strikingly similar to the coarsening dynamics of *phase ordering phenomena*, such as spinodal decomposition. In this respect, dynamics of correlations $K_{ss}(r,t)$ of the slope vector $\mathbf{V}_T = \partial \mathbf{R}_T/\partial n$ is similar to the dynamics of order parameter correlations in the phase ordering [6–8], provided $\mathbf{V}_T$ is identified as an order parameter. This identification is suggested by the scaling form of $K_{ss}(r,t)$ in Eq. (8), which, strikingly, turns out to be equivalent to the basic form for the order parameter correlations in the phase ordering processes [6–8]. Figure 2(b) gives the basic test of the self-similarity of $K_{ss}(r,t)$ as we suggested in Eq. (8). There we plot $y = K_{ss}(r,t)/K_{ss}(r=0,t)$ vs $x = r/r_1(t) = 4r/\lambda(t)$ [as before, $r_1(t) = \lambda(t)/4$ is the first zero of $K_{ss}(r,t)$]. We see that the slope-slope correlations obtained at various times indeed collapse into a single scaling function $y = \psi(x)$ [$\psi(0) = 1$, and $\psi(1) = 0$, by the construction of the rescaling procedure]. Moreover, as to standard phase ordering phenomena, our $\psi(x)$ has a pronounced oscillatory character reflecting the presence of the structural length scale $\lambda(t)$.

To qualitatively explain our numerical results, let us address the chain motion by a scaling type analysis. By (1), one has, for zero noise,

$$\frac{\partial}{\partial t}\,\mathbf{R}_T(n,t) = \frac{\partial}{\partial n}\,Be(n,t)\,\frac{\partial}{\partial n}\,\mathbf{R}_T(n,t) - \kappa\left(\frac{\partial}{\partial n}\right)^4 \mathbf{R}_T(n,t)\,, \tag{10}$$

with $e(n,t) \approx -\epsilon + \partial u/\partial n + \frac{1}{2}(\partial \mathbf{R}_T/\partial n)^2$. Here, $u(n,t)$ are longitudinal displacements, introduced by expanding $R_L(n,t) = (1-\epsilon)n + u(n,t)$ around the initial, compressed straight configuration. As the chain has fixed ends, $u = 0$ at chain's ends. Thus, $\langle \partial u/\partial n \rangle = 0$. Above we saw that the sole *long scales* at *long times* t are $\lambda(t)$ and $w(t)$, as suggested by the simulations, in particular, by the collapse of the correlation function curves in Fig. 2(b). This suggests that the typical scale for R_T is w, so $R_T \sim w$, whereas the typical scale for n is λ, so $n \sim \lambda$

and $\partial/\partial n \sim 1/\lambda$. Thus, e.g., $\partial R_T/\partial n \sim w(t)/\lambda(t)$, for a typical chain configuration in Fig. 1. Similarly, we have $\partial R_T/\partial t \sim w/t$ for a typical value of the left-hand side of Eq. (10), whereas the bending term on the right-hand side (RHS) of (10) behaves as $\sim\kappa(w/\lambda^4)$. Likewise, the first, compressional term on the RHS of (10) behaves as $\sim B(ew/\lambda^2)$. Next, we assume that, at long times, the compressional and bending terms on the RHS of Eq. (10) are of the same order. Thus,

$$w/t \sim |e|w/\lambda^2 \sim w/\lambda^4. \tag{11}$$

It follows that $\lambda \sim t^{1/4}$, i.e., $n_c = \frac{1}{4}$, and $-e \sim \lambda^{-2} \sim t^{-1/2}$, in agreement with our numerical results in Fig. 3(b). With this, for the compressional energy we find $U_{\rm com} \sim e^2 \sim t^{-1}$, in agreement with our numerical result in Fig. 3(a). Further, as $\langle e\rangle = -\epsilon + \frac{1}{2}\langle(\partial\mathbf{R}_T/\partial n)^2\rangle = -\epsilon + \frac{1}{2}[w(t)/\lambda(t)]^2 \to 0$ for $t \to \infty$, one has, at long times, $\langle(\partial\mathbf{R}_T/\partial n)^2\rangle \to 2\epsilon$, and, also, $w(t) \approx (2\epsilon)^{1/2}\lambda(t)$. Thus, as $\lambda \sim t^{n_c}$, it follows that $w \sim t^{\beta}$, with $\beta = n_c = \frac{1}{4}$, in agreement with our simulations. Finally, the bending energy $\langle U_{\rm bend}\rangle \sim \langle(\partial^2 R_T/\partial n^2)^2\rangle = w^2/\lambda^4 \sim t^{2\beta-4n_c} \sim t^{-1/2}$, in agreement with the numerical result in Fig. 3(b).

To summarize, here we have elucidated, for the first time in depth, the nature of the dynamics associated with the classical Euler instability. It is a coarsening process characterized by a growing structural length scale $\lambda \sim t^{n_c}$. At long times ($\sim L^{1/n_c}$) this length scale becomes comparable to the rod length L, and then one recovers the usual picture of a buckled rod. We reveal that the dynamics of Euler instability is similar in nature to phase ordering processes such as spinodal decomposition [6–8]: It is a stochastic coarsening process statistically self-similar in time. Like in phase ordering phenomena, stochastic dynamics here is produced by chain nonlinearities and the presence of many degrees of freedom rather than by thermal noise, which we switched off in the simulations presented here [13,14]. Associated with this coarsening process is the *growing transverse width* of the rod $w(t) \sim t^{\beta}$, with $\beta = n_c$. Such a growth of $w(t)$, with $\beta = n_c$, is strikingly similar to the interfacial coarsening processes recently found to occur in molecular beam epitaxy (so-called pyramidal or mound growth [9–11]). There, as well as in the present elastic problem, the evolving manifold (surface or line) develops a nonzero *tilt* with respect to the initial straight direction. This tilt plays a role similar to that of the order parameter in phase ordering phenomena.

We thank Andrew Karwowski and Arnaud Saint-Jalmes for discussions. This work was supported by Mylan Laboratories, Inc. and by NSF/WV EPSCoR.

[1] L. D. Landau and E. M. Lifshitz, *Theory of Elasticity* (Pergamon, New York, 1986); A. E. Love, *A Treatise on the Mathematical Theory of Elasticity* (Dover, New York, 1944).
[2] J. P. Den Hartog, *Strength of Materials* (Dover, New York, 1977).
[3] See special issue on Heteroepitaxy and Strain [Bull. Int. MRS **21**, No. 4 (1996)].
[4] L. Bordieu *et al.*, Phys. Rev. Lett. **72**, 1502 (1994).
[5] A. M. Huntz, Mater. Sci. Eng. A **201**, 211 (1995).
[6] K. Binder, Rep. Prog. Phys. **50**, 783 (1987).
[7] H. Furukawa, Adv. Phys. **34**, 703 (1985).
[8] A. J. Bray, Adv. Phys. **43**, 357 (1994).
[9] H.-J. Ernst *et al.*, Phys. Rev. Lett. **72**, 112 (1994); M. D. Johnson *et al.*, Phys. Rev. Lett. **72**, 116 (1994); W. C. Ellliott *et al.*, Phys. Rev. B **54**, 17 938 (1996); J. Amar and F. Family, Phys. Rev. B **54**, 14 742 (1996); P. Smilauer and D. D. Vvedensky, Phys. Rev. B **52**, 14 363 (1995).
[10] L. Golubović and R. P. U. Karunasiri, Phys. Rev. Lett. **66**, 3156 (1991).
[11] L. Golubović, Phys. Rev. Lett. **78**, 90 (1997).
[12] S. Edwards, Proc. Phys. Soc. London **88**, 265 (1966); L. Golubović and W. Xie, Phys. Rev. E **51**, 2856 (1995).
[13] As discussed elsewhere [14], in the presence of thermal noise (i.e., $T \neq 0$), there appears a characteristic length scale $\lambda_{\rm max} = \epsilon L_p$; here $L_p = \kappa/k_B T$ = free chain persistence length. As long as $\lambda(t) \ll \lambda_{\rm max}$, the chain dynamics is qualitatively the same as the one we described here at $T = 0$; i.e., one has a coarsening process characterized by the same coarsening exponents in Eqs. (2)–(6) as in the absence of thermal noise. At low enough T, $\lambda_{\rm max} = \epsilon L_p$ may easily exceed the size of the flexible rod. This is the case in any common mechanical engineering situation involving rodlike structures. There, rod persistence length L_p is, in any practical situation, enormously larger than the rod size. Thus, for all practical purposes of the *common* mechanical engineering, thermal noise has insignificant effects on the buckling dynamics.
[14] L. Golubović, D. Moldovan, and A. Peredera (unpublished).